HAPTICS SYMPOSIUM '16, APRIL 8–11, 2016, PHILADELPHIA, PENNSYLVANIA, USA
978-1-5090-0903-9/16/$31.00 ©2016 IEEE

Display of Needle Tip Contact Forces for Steering Guidance

Jung Hwa Bae[1] Christopher J Ploch[1] Michael A Lin[1] Bruce L Daniel[2] and Mark R Cutkosky[1]

***Abstract*— An MR-compatible biopsy needle stylet is instrumented with optical fibers that provide information about contact conditions between the needle tip and organs or hard tissues such as bone or tumors. This information is rendered via a haptic display that uses ultrasonic motors to convey directional cues to users. Lateral haptic cues at the fingertips improve the targeting accuracy and success rate in penetrating a prostate phantom. Although the original intent was for haptic cues to match the direction of contact forces and needle bending, more consistent results were obtained by using the cues as steering guidance (opposite to contact forces); accordingly this convention was adopted for the user experiments reported.**

I. INTRODUCTION

Medical robots have extended the capabilities of surgeons by enabling unprecedented surgical access and dexterity. However, teleoperated surgical systems often have the undesirable effect of preventing the surgeon from feeling what is happening. Most surgeons agree that high quality haptic sensation would increase the speed, effectiveness, and safety of teleoperated robotic surgery as well as shorten the learning curve for new surgeons learning to operate with the robot [1], [2], [3]. Augmenting the master side of surgical robots with additional haptic feedback is a promising way to restore these missing sensations, and may even allow new information to be conveyed that surgeons have not had access to before.

While it is possible to obtain physical information about the tool-tissue interaction by adding a force sensor or accelerometer to the base of the tool [4], the forces acting on the tool tip are masked by friction forces from the intervening tissue, especially in the case of a long needle [5], [6]. Therefore, the ability to sense the forces on the tip of a needle provides an interesting case to explore the possible benefits of augmented haptic feedback in minimally invasive interventions.

Previously, we built a tip-force sensing biopsy needle instrumented with optical fiber Bragg grating (FBG) strain sensors and demonstrated that high-frequency axial tip-force information can improve the success rate of membrane puncture detection [7]. In addition to high-frequency information, we believe that low-frequency tip-tissue interaction force feedback is important for surgical tasks, such as tumor identification by comparing tissue stiffness, and when driving the needle to a target during a biopsy. In this paper, we demonstrate the ability of low frequency directional tactile feedback to help in a needle positioning and puncture task by comparing a system with a direct, low friction mechanical connection to the needle (analogous to a passive teleoperator,

[1]Mechanical Engineering Dept., Stanford University, Stanford, USA jbae7@stanford.edu
[2]Radiology Dept., Stanford Hospital, Stanford, USA

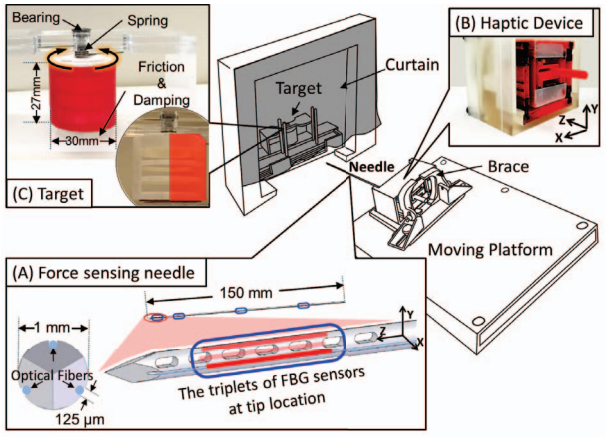

Fig. 1. Experiment setup consists of a needle instrumented with optical fibers (A) and a pen-like haptic device (B) mounted on a 3-DOF rolling platform. Users manipulate the platform and needle with the goal of puncturing a target (C) occluded by a curtain. The target rotates, evading puncture, if the needle is not accurately aligned.

e.g., [8]) to the performance of the same system with added haptic steering cues based on measured needle tip forces.

While various haptic modalities could convey directional low-frequency information from the tip of a needle to the surgeon, we believe that fingertip skin deformation feedback from a pen-like interface shows promise as an especially intuitive means of communication. This is because we found through interviews at the Stanford Medical School that surgeons in particular often use a pen grasp when performing biopsies. Furthermore, the ability for skin deformation to effectively communicate directional information with low forces and only a few millimeters of displacement [9], [10], [11] makes it ideal for integration into compact, low-power haptic feedback modules that could be used in a surgical setting. Furthermore it is easily applied to a purely mechanical or pneumatic teleoperation system [8], [12].

Using this newly designed haptic device for the tip-force sensing needle, we found that lateral tip-force information significantly improved performance in a task simulating a biopsy procedure.

II. METHODS AND MATERIALS

To explore how lateral tip-force information affects a targeting task, we built the apparatus shown in Fig.1. The user rests his or her hand on a freely moving platform that can translate and rotate in the plane. A needle (Fig.1A) and lightweight haptic display (B) are attached to the platform. The platform is a planar analog to a passive teleoperation system for manipulating a needle. It permits forces on the needle to be transmitted directly to the user (especially axial

forces, as the needle is much stiffer in compression than in bending), but with some masking due to inertia and a small amount of friction.

The target (Fig.1C) is meant to simulate a prostate, including the outer membrane. It consists of a cylinder covered with a thin layer of ripstop nylon tape. Unless the needle tip is aligned with the central axis of the target, the cylinder rotates away, evading puncture. A curtain is placed just above the plane of the needle to hide the target from view.

In operation, a user grasps the haptic display with the thumb and index finger while resting his or her hand upon the platform. The hand pushes the platform, guiding the needle into contact with the target. When interaction forces are detected at the tip of the needle, the haptic display presses upon the user's fingertips providing additional feedback.

A. Needle Description

A biopsy needle capable of detecting tip contact forces was created by embedding three optical fibers in grooves along the inner stylet of an off-the-shelf 18 gauge MR-compatible needle. The grooves are spaced 120° apart in the needle cross-section, as shown in Fig.1A. Each fiber contains four FBG sensors along its length, so that there are four triplets of FBGs, each at a different location along the needle, capable of measuring axial and bending strains. The triplet nearest the tip, where bending moments are very small, can accurately measure (x,y,z) tip contact forces. Slotted features at the needle tip improve sensitivity to axial strain.

A calibration matrix calculated in [7] converts strain readings from the optical sensors to triaxial forces at the tip of the needle. The minimum lateral force that can be sensed by the tip FBGs is 4 mN, with a maximum frequency of 500 Hz [5], which is sufficient to capture interaction forces in the human sensible frequency range (0-400 Hz) [13]. The FBG sensors are read with a Micron optics sm-130 interrogator at 1 kHz.

B. Phantom Materials

As noted above, the simulated biopsy target is a hollow cylinder covered with ripstop nylon tape. The cylinder has a small rotary damper to prevent it from spinning too freely and a torsional spring (0.43 Nm/rad) to restore it to its equilibrium orientation. Although an actual prostate can both translate and rotate [14], [15], the current setup was judged by physicians to present an equivalent level of difficulty for membrane puncture.

In front of the target cylinder, a layer of "extra firm" tofu (bean curd) simulates the effect of soft intervening tissue [16], which the needle must traverse on its way to the target. This material was adopted after determining that synthetic elastomers and foams presented a less convincing simulation. The tofu and the cylinder's ripstop tape are replaced frequently.

C. Haptic Display Apparatus

1) Device Design: The haptic feedback device presents a knob, which users grasped with their fingertips. The backs of the fingertips where supported by a pair of external braces, while the rest of the hand was supported by the moving platform, as shown in Fig.2.

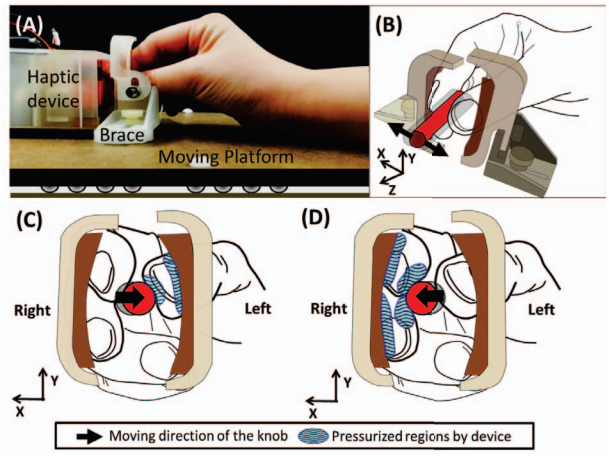

Fig. 2. Subjects displace the moving platform to manipulate the needle while they interact with the haptic device (A). The haptic device imparts small lateral motions to a knob (B) which presses the subjects finger tips against braces. Subjects use the skin deformation cues on their finger pads (C,D) to interpret what happens at the needle tip.

To impart motions, we adapted a flexure mechanism presented in [17] as shown in Fig.3. In order to translate the rotational motions of the motors to small translational motions, the flexure contains two stages, one for x motions and one for y motions. A pin, offset from the shaft of each motor, travels in a slot on its associated stage (similar to a sotch yoke mechanism). Whereas [17] used the flexure to generate 2-DOF lateral skin stretch, we are using a scaled-up version to apply larger forces to the fingertips corresponding to the two components of lateral contact forces sensed by the needle tip. In particular, the feedback produces normal and lateral skin deformation cues at the finger pads as well

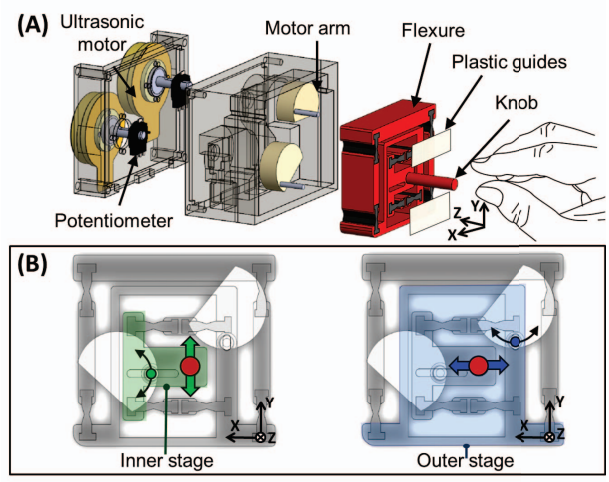

Fig. 3. (A) Exploded view of the haptic device shows the arrangement of the ultrasonic motors, motor arms and flexure mechanism that enables Cartesian position control of the knob. (B) shows independent stages that two motors actuate with pins in slots to achieve position control in the x and y directions.

as pressure on the finger pads and nails when the fingers are pressed by the laterally translating knob against the surrounding braces. These finger pad deformations are intended to be similar to those that occur naturally during interactions with pen-like tools when lateral forces are applied at the tip. The knob can move a maximum of ± 3 mm in either direction with about 10 N of force.

The flexure was printed with a 3D Printer[1], using polylactic acid (PLA) for the stiff components and thermoplastic elastomer (TPE) for the compliant components. Finite element analysis was performed in Solidworks to ensure that the two dimensions of the flexure had similar spring constants of approximately 1000 N/m. Nonplanar motion was minimized by adding additional plastic guides on top of the flexure, as seen in Fig.3.

2) Device Actuation: We chose Shinsei USR-30 piezoelectric ultrasonic motors to actuate the haptic feedback device because they are compact and high-torque, and MR-compatible variants are available. These actuators have been used in MR-compatible medical robotic systems in the past for these reasons [18], [19], [20]. They also run very smoothly with no perceivable vibration, unlike most RC servos, making them a good fit for haptic applications. Their high torque capability makes gearing unnecessary for our application. Rotary potentiometer position sensors[2] were added to the motor shafts to close the position control loop. The signal to noise ratio of the potentiometer is 0.001 and its average noise amplitude is 0.3°, which corresponds to a 0.043 mm displacement resolution.

One drawback of the ultrasonic motor is that it is not backdrivable [21]. This is often undesirable for haptic devices, which are usually impedance-type with low inertia and gearing. Our actuators are closer to those used in admittance-type haptic devices, which require force sensing to function. However, in the present case we are using the motors only for position control, to deform the finger pads so as to provide position cues and the resulting pressure cues that are representative of forces sensed by the needle tip.

A second drawback of ultrasonic motors is the presence of a velocity deadband [22], [23], which hinders the smooth position control, especially at low speeds and small displacements. Although sophisticated methods have been developed to compensate for this deadband, including a differential gear system using two ultrasonic motors to control one degree of freedom [24], fuzzy control schemes [25], and neural networks [26], we chose to use a simpler approach that is adequate for this position-controlled implementation. This involved first shifting the deadband velocity from a nonzero magnitude to zero by tuning the motor velocity range setting on the Shinsei motor driver. Then, by applying a threshold voltage to the input of the ultrasonic motors, we were able to achieve a more linear controllable speed (Fig.4).

While the deadband threshold can vary with the load on the motor, we assumed the impedance from the flexure and fingerpads over such small displacements ($\pm 3\,mm$) was small enough to ignore, and noticed no performance issues from doing so. Position control results with the flexure in place are seen in Fig.5 for a smooth 0.5 Hz sinewave.

[1]Flashforge Creator Pro

[2]Panasonic EVW-AE4001B14

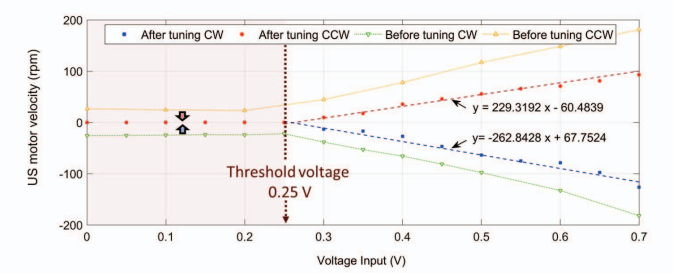

Fig. 4. Ultrasonic motor speed characterization. After tuning the ultrasonic motor driver, the deadband velocity becomes zero over a voltage range of 0-0.25V.

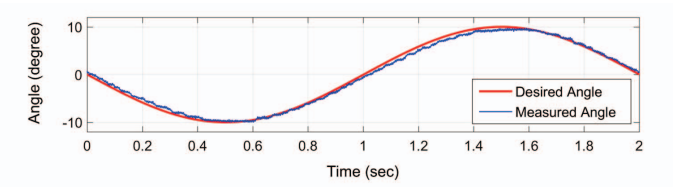

Fig. 5. Motor position control result after adjusting velocity deadband with flexure in place.

As noted earlier, useful haptic information ranges from approx 0-400 Hz. However, the focus in this implementation is to provide relatively low frequency and low magnitude directional cues. This is because higher frequency information tends to lose its directional information content as it becomes vibratory (normal skin deformation can be felt from 0-30 Hz; directional skin stretch is felt from 0-15 Hz [27]), and could be added later with an additional actuator to complement the directional feedback [28]. We tested the frequency response of the ultrasonic motor flexure system for a series of commanded sine waves to determine its frequency capabilities. The resulting bandwidth for an input amplitude of approximately 10° is 22.5 Hz, as shown in Fig.6.

Force amplitude and direction information read from the tip of the needle are linearly mapped to the displacement of the knob, x_{knob}. The following equations relate sensed forces, F_x and F_y, to the motor positions.

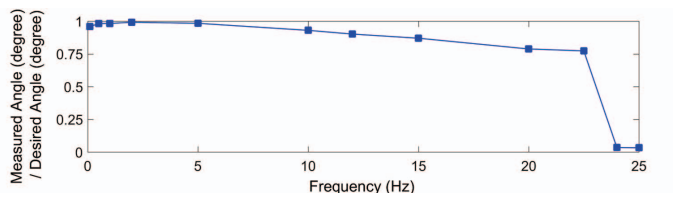

Fig. 6. Frequency response of the ultrasonic motors after deadband velocity adjustment, measured by giving a series of $\pm 10^\circ$ sinusoidal commands to the motors.

$$x_{knob} = F_x C_{fd} \quad (1)$$

$$y_{knob} = F_y C_{fd} \quad (2)$$

$$\theta_{Xmotor} = \theta_0 + \sin^{-1}(x_{knob}/r) \quad (3)$$

$$\theta_{Ymotor} = \theta_0 + \sin^{-1}(y_{knob}/r) \quad (4)$$

where x_{knob} and y_{knob} are the displacements of the knob in the x and y directions (Fig.3) respectively, θ_0 is the home position of the motor at zero displacement, and r is the offset distance between the motor shaft and the pin of the scotch-yoke mechanism in the haptic device. The value of C_{fd} was chosen based on pilot user experiments. Subjects indicated that they had difficulty in sensing the axial forces naturally transmitted through the needle and moving plate when the lateral haptic cues were too large. Based on this observation, we decided to keep the factor small to conserve axial sensitivity. However, we chose a large enough value for C_{fd} that subjects could still correctly identify the direction of displacement when feedback was provided. We obtained an initial estimate of a minimum displacement through a pilot test with five subjects. Subjects were able to identify the direction of 0.1 mm displacements with an average accuracy of 90%.

3) Communication: Tight integration of our sensing system and haptic device is crucial for our application because needle interaction forces must be sensed and relayed with no perceptible delay. Delays between an event and the corresponding haptic stimulus start to become noticeable when they are larger than 45 ms[29], [30]. Keeping this delay small is especially important in our case as axial contact forces are transmitted directly along the needle shaft and into the moving platform.

Our communication system consists of two ethernet boards, one for reading the interrogator (tip-force sensing data) and another dedicated to a Linux based EtherCAT system used for controlling the motors. By setting the execution priorities in the C++ program, we were able to build a soft real time system. To minimize the delay from the interrogator, we used an unbuffered data collection function from the sm-130 interrogator API[3] to read wavelength data. We then calculated the lateral forces using a calibration matrix. The forces are linearly mapped to desired displacements, which are further mapped to the corresponding motor angles. A proportional-integral controller is used to achieve the desired motor positions. The average latency between the sensed strain data and the position feedback output was measured for a 1 kHz acquisition speed, and was found to be approximately 36 ms, which is within our desired range. Fig.7 shows the delay between sensing and actuation as the needle tip is tapped twice from the right.

III. EXPERIMENT PROCEDURE

In order to test the potential for the augmented directional feedback system to improve surgical procedures, we designed a task that simulates a prostate biopsy. Ten subjects were each instructed to puncture a prostate phantom 20 separate times by steering the moving platform and needle with their hands.

As noted in the previous section, a curtain hid the target from view. The target was randomly positioned ± 6 cm to the left of right for each trial so that the needle was never aligned perfectly with the target and its position was not predictable. The intervening tissue phantom (extra firm tofu) was replaced after each attempt, and the membrane was replaced between trials, so that repeated punctures would not reduce the difficulty of the task over time. Half of the trials were given with augmented haptic feedback and half without, again distributed randomly. To simplify the experiment, forces were only sensed and displayed in the x direction, as shown in Fig.9. Due to the cylindrical shape of the target, forces in the y direction were not particularly useful.

The haptic feedback displayed to the subject is opposite

[3]Micron Optics Inc., Atlanta, GA, USA

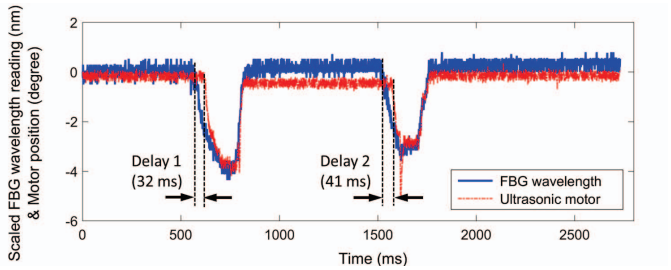

Fig. 7. Haptic device system delay between FBS sensor data at the needle tip and position data of the ultrasonic motor. Average delay was 36ms.

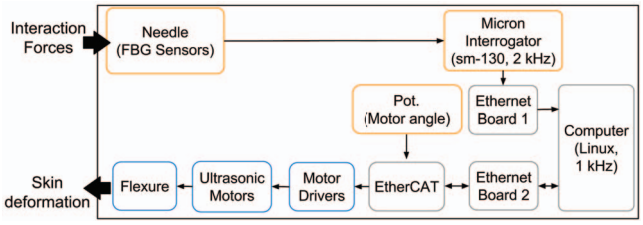

Fig. 8. Haptic device system communication schematic

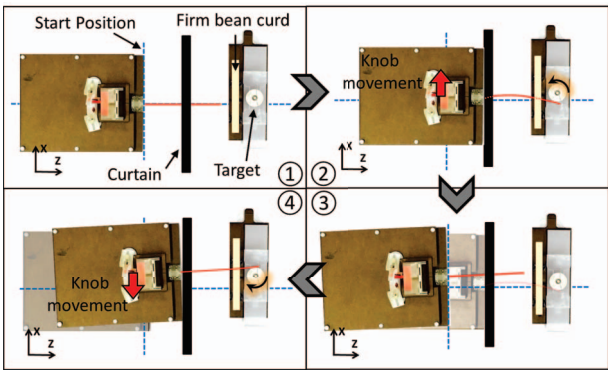

Fig. 9. Typical starting sequence: (1) initial position; (2) first attempt to penetrate target (needle deflects in -x direction, feedback applied in opposite direction); (3) user retracts needle and reorients; (4) second attempt results in needle deflected in +x direction with feedback in -x direction.

to the direction that the target deflects the needle and proportional to the deflection. As a result, it directs the subject toward the center of the cylinder. Subjects were instructed to view the feedback as directional guidance information. Fig.9 illustrates a typical starting sequence: (1) the subject pushes the needle forward, but the needle is not aligned with the target center; (2) the needle deflects in the -x direction so that haptic feedback is applied in the +x direction; (3) the subject corrects by tilting the needle and trying again; (4) the subject has over-corrected so that the needle now deflects in the +x direction and feedback is applied in the -x direction.

For each trial, a subject was allowed ten attempts to puncture, with each attempt consisting of driving the needle toward the target and then removing it. After each attempt, the following information was verbally collected from the subject: (i) whether they believe they punctured the membrane of the target, (ii) whether they thought the needle was to the left or right of the target center, and (iii) whether they were confident of each of the previous two answers. Between attempts, the subjects were instructed to make lateral position corrections based on the previous attempt to align the needle with the center of the target as well as they could. All tests were conducted in accord with IRB Protocol 26526.

IV. RESULTS

Experiments were conducted with 10 subjects, (8 male, 2 female) with ages ranging from 23 to 29. Among these, 4 had experience in haptics and none had prior experience in needle procedures. Of the 20 puncture trials (maximum 10 attempts to puncture for each trial) required of each subject, the average number of attempts to puncture in the case of no added feedback was 4.75 with a standard deviation of 1.32, while the average with feedback was 3.13, with a standard deviation of 0.53, as seen in Figure 8. We performed a one-tailed paired t-test with the following null hypothesis: (*average number of attempts without feedback - with feedback*)>0. The result shows a statistically significant difference (p-value= 0.0028) with Bonferroni correction $p<0.005$.

Another metric for performance of the device was how accurate the subjects were at determining where the needle tip was with respect to the target (Fig. IVB). With directional feedback, subjects reported the correct needle location 61.8% of the time with a variance of 0.03 (3%). Without the additional feedback, subjects were correct 46.8% of the time with a variance of 0.012 (1.2%). A one tail paired t-test shows a statistically significant difference (p-value= 0.0041) with Bonferroni correction $p<0.005$. There were large differences between subjects in terms of how well they utilized the feedback, with one subject achieving 93% accuracy at direction determination, while the lowest accuracy was 30%.

V. DISCUSSION

Results indicate that directional fingertip haptic feedback successfully reduced the number of attempts needed to puncture the membrane. The direction identification accuracy improved greatly for some subjects, while others did not improve, showing that the device worked well for some, but not all, subjects.

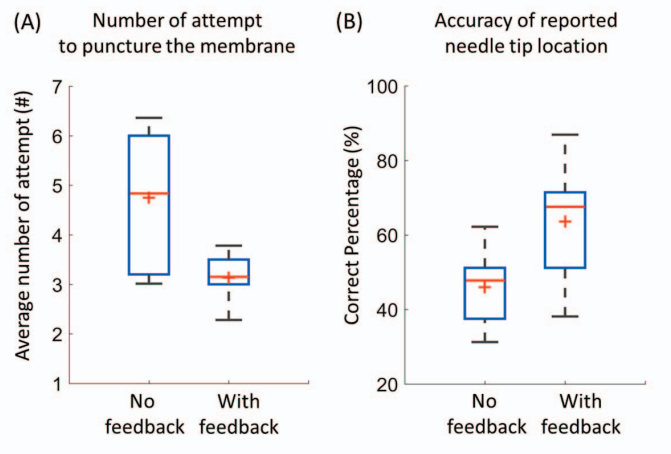

Fig. 10. (A) Number of attempts before puncturing the target membrane. (B) Accuracy of subject-reported needle tip location with respect to the target. Boxes represent 25-75% of data, + mark is the median, line is the average. Whiskers show data between 10-90%.

In general, puncturing the nylon membrane was challenging because it required significant axial force and the cylinder rotated easily if the needle was off-center. However, subject performance improved rapidly, showing that a significant training effect existed. Randomizing the trials was therefore important. Our haptic feedback device did not augment axial force or provide high frequency feedback associated with puncturing membranes, both of which could have made the task easier. However, the focus of the task was to test how well lateral force feedback can help users locate the best place to puncture, as opposed to how well they could actually execute the puncture. The metrics convincingly show that the feedback helped locate the center of the prostate phantom.

One interesting issue raised during the pilot phase of this experiment was whether users preferred feedback in the same direction as the tip load or in the opposite direction. Our initial thought was to provide feedback in the same direction, thinking that it should feel as if the surgeons fingers are at the tip of the needle and experiencing exactly the same forces. However, when we tested this style of feedback, the results were not uniform. Some subjects understood the feedback well, while others became confused or always responded in the opposite way from what was expected. This result may arise from users perceiving the haptic feedback as corresponding to a reaction force felt at the base of the needle instead of the contact force at the tip. To sidestep these issues and improve consistency, we decided to adopt the convention that the feedback is a guidance force pointing toward the ideal puncture location based on sensing data – a simpler concept to grasp.

VI. CONCLUSIONS AND FUTURE WORK

Subjects could easily determine the direction in which haptic feedback was guiding them, and the guidance clearly improved their task performance. The puncturing element of the task might have been easier if the haptic device also

provided augmented axial feedback to the subjects, which could be a useful addition for future experiments. Adding a third degree of freedom should further increase realism and allow for experiments using biological phantoms with more complicated geometries. Corresponding experiments are being planned using subjects experienced in needle procedures.

Another reasonable modification would be to replace the ultrasonic motors with actuators that have lower impedance, so that we can truly transmit dynamic forces instead of positions. This will likely increase the intuitiveness of the feedback and perhaps reduce some of the confusion that arose when subjects were told to interpret the feedback as a force felt by the needle tip. Electroactive polymer artificial muscles show promise as a way to achieve true impedance control while keeping the device MR-compatible.

Finally, a high frequency actuator (e.g. as in [4]) could be added to complement the low frequency skin deformation. This would increase the perception of puncture events, texture of tissue, and impacts.

ACKNOWLEDGMENT

We thank Daniel Shin for his support to ideate the haptic device designs and pilot tests. This work has been supported by NIH PO1 CA159992, NIH SBIR R43-EB011822, and a Kwanjeong Scholarship.

REFERENCES

[1] T. N. Judkins, D. Oleynikov, and N. Stergiou, "Enhanced robotic surgical training using augmented visual feedback," *Surgical innovation*, vol. 15, no. 1, pp. 59–68, 2008.

[2] J. K. Koehn and K. J. Kuchenbecker, "Surgeons and non-surgeons prefer haptic feedback of instrument vibrations during robotic surgery," *Surgical endoscopy*, pp. 1–14, 2014.

[3] C. E. Reiley, T. Akinbiyi, D. Burschka, D. C. Chang, A. M. Okamura, and D. D. Yuh, "Effects of visual force feedback on robot-assisted surgical task performance," *The Journal of thoracic and cardiovascular surgery*, vol. 135, no. 1, pp. 196–202, 2008.

[4] K. J. Kuchenbecker, J. Gewirtz, W. McMahan, D. Standish, P. Martin, J. Bohren, P. J. Mendoza, and D. I. Lee, "Verrotouch: high-frequency acceleration feedback for telerobotic surgery," in *Haptics: Generating and perceiving tangible sensations*. Springer, 2010, pp. 189–196.

[5] S. Elayaperumal, J. H. Bae, D. Christensen, M. R. Cutkosky, B. L. Daniel, R. J. Black, J. M. Costa, F. Faridian, and B. Moslehi, "Mr-compatible biopsy needle with enhanced tip force sensing," in *WHC, 2013*. IEEE, 2013, pp. 109–114.

[6] H. Kataoka, T. Washio, K. Chinzei, K. Mizuhara, C. Simone, and A. M. Okamura, "Measurement of the tip and friction force acting on a needle during penetration," in *MICCAI 2002*. Springer, 2002, pp. 216–223.

[7] S. Elayaperumal, J. H. Bae, B. L. Daniel, and M. R. Cutkosky, "Detection of membrane puncture with haptic feedback using a tip-force sensing needle," in *IROS 2014, 2014 IEEE/RSJ International Conference on*. IEEE, 2014, pp. 3975–3981.

[8] S. Elayaperumal, M. R. Cutkosky, P. Renaud, and B. L. Daniel, "A passive parallel master–slave mechanism for magnetic resonance imaging-guided interventions," *Journal of medical devices*, vol. 9, no. 1, p. 011008, 2015.

[9] Z. F. Quek, S. Schorr, I. Nisky, W. Provancher, and A. M. Okamura, "Sensory substitution using 3-degree-of-freedom tangential and normal skin deformation feedback," in *HAPTICS, 2014 IEEE*. IEEE, 2014, pp. 27–33.

[10] B. T. Gleeson, S. K. Horschel, and W. R. Provancher, "Communication of direction through lateral skin stretch at the fingertip," in *EuroHaptics conference, 2009 and Symposium on Haptic Interfaces for Virtual Environment and Teleoperator Systems. World Haptics 2009. Third Joint*. IEEE, 2009, pp. 172–177.

[11] B. T. Gleeson, S. K. Horschel, and W. R. Provancher, "Perception of direction for applied tangential skin displacement: Effects of speed, displacement, and repetition," *Haptics, IEEE Transactions on*, vol. 3, no. 3, pp. 177–188, 2010.

[12] A. Elmasry and M. Liermann, "Passive pneumatic teleoperation system," in *ASME/BATH 2013 Symposium on Fluid Power and Motion Control*. American Society of Mechanical Engineers, 2013, pp. V001T01A040–V001T01A040.

[13] R. S. Johansson and J. R. Flanagan, "Coding and use of tactile signals from the fingertips in object manipulation tasks," *Nature Reviews Neuroscience*, vol. 10, no. 5, pp. 345–359, 2009.

[14] V. Lagerburg, M. A. Moerland, J. J. Lagendijk, and J. J. Battermann, "Measurement of prostate rotation during insertion of needles for brachytherapy," *Radiotherapy and Oncology*, vol. 77, no. 3, pp. 318–323, 2005.

[15] N. N. Stone, J. Roy, S. Hong, Y.-C. Lo, and R. G. Stock, "Prostate gland motion and deformation caused by needle placement during brachytherapy," *Brachytherapy*, vol. 1, no. 3, pp. 154–160, 2002.

[16] J. Wu, "Tofu as a tissue-mimicking material," *Ultrasound in medicine & biology*, vol. 27, no. 9, pp. 1297–1300, 2001.

[17] B. T. Gleeson, S. K. Horschel, and W. R. Provancher, "Design of a fingertip-mounted tactile display with tangential skin displacement feedback," *Haptics, IEEE Transactions on*, vol. 3, no. 4, pp. 297–301, 2010.

[18] M. S. Judenhofer, C. Catana, B. K. Swann, S. B. Siegel, W.-I. Jung, R. E. Nutt, S. R. Cherry, C. D. Claussen, and B. J. Pichler, "Pet/mr images acquired with a compact mr-compatible pet detector in a 7-t magnet 1," *Radiology*, vol. 244, no. 3, pp. 807–814, 2007.

[19] H. Elhawary, A. Zivanovic, M. Rea, B. L. Davies, C. Besant, I. Young, M. Lamperth, *et al.*, "A modular approach to mri-compatible robotics," *Engineering in Medicine and Biology Magazine, IEEE*, vol. 27, no. 3, pp. 35–41, 2008.

[20] B. Maurin, B. Bayle, J. Gangloff, P. Zanne, M. de Mathelin, and O. Piccin, "A robotized positioning platform guided by computed tomography: Practical issues and evaluation," in *Robotics and Automation, 2006. ICRA 2006. Proceedings 2006 IEEE International Conference on*. IEEE, 2006, pp. 251–256.

[21] A. Erwin, M. K. O'Malley, D. Ress, and F. Sergi, "Development, control, and mri-compatibility of the mr-softwrist," in *ICORR, 2015 IEEE International Conference on*. IEEE, 2015, pp. 187–192.

[22] S.-i. Furuya, T. Maruhashi, Y. Izuno, and M. Nakaoka, "Load-adaptive frequency tracking control implementation of two-phase resonant inverter for ultrasonic motor," *Power Electronics, IEEE Transactions on*, vol. 7, no. 3, pp. 542–550, 1992.

[23] J. Wallaschek, "Contact mechanics of piezoelectric ultrasonic motors," *Smart materials and Structures*, vol. 7, no. 3, p. 369, 1998.

[24] C. M. Esser, C. Parthiban, and M. R. Zinn, "Development of a parallel actuation approach for mr-compatible robotics," *Mechatronics, IEEE/ASME Transactions on*, vol. 19, no. 3, pp. 904–915, 2014.

[25] T. Senjyu, T. Yoshida, K. Uezato, and T. Funabashi, "Position control of ultrasonic motors using adaptive backstepping control and dead-zone compensation with fuzzy inference," in *Industrial Technology, 2002. IEEE ICIT'02. 2002 IEEE International Conference on*, vol. 1. IEEE, 2002, pp. 560–565.

[26] T. Senjyu, H. Miyazato, S. Yokoda, and K. Uezato, "Speed control of ultrasonic motors using neural network," *Power Electronics, IEEE Transactions on*, vol. 13, no. 3, pp. 381–387, 1998.

[27] R. D. Howe, "Tactile sensing and control of robotic manipulation," *Advanced Robotics*, vol. 8, no. 3, pp. 245–261, 1993.

[28] K. Bark, W. McMahan, A. Remington, J. Gewirtz, A. Wedmid, D. I. Lee, and K. J. Kuchenbecker, "In vivo validation of a system for haptic feedback of tool vibrations in robotic surgery," *Surgical endoscopy*, vol. 27, no. 2, pp. 656–664, 2013.

[29] I. M. Vogels, "Detection of temporal delays in visual-haptic interfaces," *Human factors: The journal of the Human Factors and Ergonomics society*, vol. 46, no. 1, pp. 118–134, 2004.

[30] A. J. Doxon, D. E. Johnson, H. Z. Tan, and W. Provancher, "Human detection and discrimination of tactile repeatability, mechanical backlash, and temporal delay in a combined tactile-kinesthetic haptic display system," *Haptics, IEEE Transactions on*, vol. 6, no. 4, pp. 453–463, 2013.